

# On the Smoothness of Nonlinear System Identification <sup>★</sup>

Antônio H. Ribeiro <sup>a,c</sup>, Koen Tiels <sup>c</sup>, Jack Umenberger <sup>c</sup>, Thomas B. Schön <sup>c</sup>,  
Luis A. Aguirre <sup>b</sup>

<sup>a</sup>Graduate Program in Electrical Engineering, Universidade Federal de Minas Gerais, Av. Antônio Carlos 6627, 31270-901, Belo Horizonte, Brazil

<sup>b</sup>Dept. of Electronic Engineering, Universidade Federal de Minas Gerais, Av. Antônio Carlos 6627, 31270-901, Belo Horizonte, Brazil

<sup>c</sup>Dept. of Information Technology, Uppsala University, 751-05 Uppsala, Sweden

---

## Abstract

New light is shed onto optimization problems resulting from prediction error parameter estimation of linear and nonlinear systems. It is shown that the “smoothness” of the objective function depends both on the simulation length and on the decay rate of the prediction model. More precisely, for regions of the parameter space where the model is not contractive, the Lipschitz constant and  $\beta$ -smoothness of the objective function might blow up exponentially with the simulation length, making it hard to numerically find minima within those regions or, even, to escape from them. In addition to providing theoretical understanding of this problem, this paper also proposes the use of multiple shooting as a viable solution. The proposed method minimizes the error between a prediction model and observed values. Rather than running the prediction model over the entire dataset, as in the original prediction error formulation, multiple shooting splits the data into smaller subsets and runs the prediction model over each subdivision, making the simulation length a design parameter and making it possible to solve problems that would be infeasible using a standard approach. The equivalence with the original problem is obtained by including constraints in the optimization. The method is illustrated for the parameter estimation of nonlinear systems with chaotic or unstable behavior, as well as on neural network parameter estimation.

*Key words:* Prediction error methods, multiple shooting, system identification, output error models, parameter estimation, dynamic systems.

---

## 1 Introduction

Prediction error methods [1] are a widespread class of methods for parameter estimation of dynamic models. They are used for modeling a wide variety of systems such as unmanned helicopters [2], the downhole pressure of oil wells [3], geosynchronous orbits [4], daily groundwater levels [5], the voltage of fuel cells [6] and magnetic disturbances near earth [7]. While the classical literature focuses primarily on the estimation of linear systems [1], the framework is general and it enjoys appealing asymptotic properties for the general nonlinear setup [8].

The principle behind prediction error methods is to estimate the parameters of dynamic models by minimizing the error between predicted and measured trajectories. Many well known estimation methods fit into this framework, such as the minimization of the one-step-ahead prediction error and of the free-run-simulation error.

---

<sup>★</sup> This work has been supported by the Brazilian agencies CAPES - Coordenação de Aperfeiçoamento de Pessoal de Nível Superior (Finance Code: 001), CNPq - Conselho Nacional de Desenvolvimento Científico e Tecnológico (contract number: 302079/2011-4, 200931/2018-0 and 142211/2018-4) and FAPEMIG - Fundação de Amparo à Pesquisa do Estado de Minas Gerais (contract number: TEC 1217/98), by the Swedish Research Council (VR) via the projects *NewLEADS - New Directions in Learning Dynamical Systems* (contract number: 621-2016-06079) and *Learning flexible models for nonlinear dynamics* (contract number: 2017-03807), and by the Swedish Foundation for Strategic Research (SSF) via the project *ASSEMBLE* (contract number: RIT15-0012).

Email address: antonio-ribeiro@ufmg.br (Antônio H. Ribeiro).

URL: antonior92.github.io (Antônio H. Ribeiro).

While minimizing the one-step-ahead prediction usually yields an easier optimization problem, models minimizing the free-run simulation error or other recurrent structures may produce more accurate models. These recurrent models often have smaller generalization error [9], [10] and better capability of long-term prediction [11], [12]. Minimizing recurrent structures is used, for instance, to improve the model structure selection of polynomial models [13] [14], fine-tune parameters of nonlinear state-space [15] and block-oriented models [16] and to provide, in several situations, more accurate neural network [17], [18], polynomial and rational models [17].

It is common knowledge among practitioners that the optimization problem resulting from a recurrent model structure is harder to solve [13]. For linearly parametrized models and convex loss functions, minimization of one-step-ahead prediction error leads to a convex optimization problem; for recurrent model structures, the ensuing optimization is, in general, non-convex, complicating the search for global optima. Even during local optimization, recurrent model structures can lead to cost functions with poor smoothness properties, including many ‘jagged’ local minima, cf. Figure 2 for an illustration. Understanding of the relationship between model structure and smoothness properties of the cost function is, however, imprecise and provides little insight into ways to circumvent the problem. Furthermore, the few studies that investigate the objective function properties in this context are focused on linear systems [19].

The purpose of this paper is twofold. First, we aim to provide insight into the properties of the objective function arising in prediction error estimation problems in a general nonlinear setup. Specifically, we show how the smoothness of the objective function depends on two factors: the simulation length and the decay rate of the recurrent part of the prediction model. Second, we leverage these theoretical insights for the design of methods that make the optimization problem easier to solve.

To realize the second objective we apply, in the context of prediction error methods, the *multiple shooting* technique. The multiple shooting formulation has reportedly provided improvements in the parameter estimation of ordinary differential equations [20], [21], [22], [23], [24], [25], in the solution of optimal control [26], [27], [28] and two-point boundary value problems [29]. In a system identification setting, multiple shooting has been used for estimating polynomial nonlinear space-state models [30] and output error models [31] in settings where conventional methods fail to provide good solutions. And, here, we extend the class of system identification problems for which multiple shooting can be applied to the entire class of prediction error methods. In addition, theoretical arguments are put forward to help understand why and when the proposed method is

useful.

The outline of the paper is the following: Section 2 gives a unified view of prediction error methods in a fully nonlinear setting. Section 3 provides results about the objective function’s Lipschitzness and  $\beta$ -smoothness for problems with a recurrent prediction model. Section 4 presents a multiple shooting formulation for prediction error methods and analyzes its objective function properties. Section 5 describes a multiple shooting implementation and gives numerical examples. Final comments and future work are provided in Section 6.

## 2 Prediction error methods

While prediction error methods are widely known they are usually introduced from a linear perspective [1]. In this section, we present them in a fully nonlinear framework. The results presented in the remainder of the paper hold in this general nonlinear framework.

### 2.1 Notation and Setup

Consider the dataset  $\mathcal{Z}^N = \{(\mathbf{u}[k], \mathbf{y}[k]), k = 1, 2, \dots, N\}$  containing measured inputs and outputs of a dynamical system. Here  $\mathbf{u}[k] \in \mathbb{R}^{N_u}$  and  $\mathbf{y}[k] \in \mathbb{R}^{N_y}$  are vectors of inputs and outputs at an instant  $k$ . We consider  $\mathbf{y}[k]$  and  $\mathbf{u}[k]$  to be one realization of the vector random variables  $\mathbf{Y}[k]$  and  $\mathbf{U}[k]$ . We assume that the underlying dynamics can be approximated by a finite-order system and that  $\mathbf{Y}[k]$  depends only on a finite number of past inputs and auto-regressive terms:

$$\begin{aligned}\underline{\mathbf{U}}[k] &= [\mathbf{U}[k], \dots, \mathbf{U}[k - n_u]], \\ \underline{\mathbf{Y}}[k - 1] &= [\mathbf{Y}[k - 1], \dots, \mathbf{Y}[k - n_y]],\end{aligned}$$

where  $n_y, n_u$  are the maximum input and output lags. The measured values of those random vectors are denoted by  $\underline{\mathbf{u}}[k]$  and  $\underline{\mathbf{y}}[k - 1]$ , respectively.

### 2.2 Framework

Prediction error methods assume a parameterized model for the dynamic system, with the model behavior depending on a parameter vector  $\boldsymbol{\theta}$ . In *practice*, the parameter vector is estimated by minimizing the distance between the model predicted output  $\hat{\mathbf{y}}[k]$  and the measured value  $\mathbf{y}[k]$ :

$$V = \frac{1}{N} \sum_{k=1}^N \|\mathbf{y}[k] - \hat{\mathbf{y}}[k]\|^2. \quad (1)$$

Here, we use a state-space representation. Hence, the predicted output  $\hat{\mathbf{y}}$  is defined by the equations:

$$\begin{aligned}\mathbf{x}[k] &= \mathbf{h}(\mathbf{x}[k-1], \mathbf{z}[k]; \boldsymbol{\theta}), \text{ for } \mathbf{x}[0] = \mathbf{x}_0. \\ \hat{\mathbf{y}}[k] &= \mathbf{g}(\mathbf{x}[k], \mathbf{z}[k]; \boldsymbol{\theta}),\end{aligned}\quad (2)$$

where  $\mathbf{x}[k]$  denotes the state vector at instant  $k$  and  $\mathbf{z}[k] = (\mathbf{u}[k], \mathbf{y}[k-1])$ . Notice that  $\mathbf{z}[k]$  contains both measured input *and* output values. This is the most general setup, and allows us to include nonlinear ARX and ARMAX models in the presented framework (see Section 2.4). It is, also, the representation of choice for some grey-box models [32]. Notice that the prediction  $\hat{\mathbf{y}}[k]$  depends upon  $\boldsymbol{\theta}$  and  $\mathbf{x}_0$  although such a dependence is not made explicit in the notation. Representation (2) will be called the *prediction model*.

### 2.3 Estimator properties

In this section, we explain some basic properties of prediction error methods. In order to do so, we define the optimal prediction of  $\mathbf{y}[k]$  as the following conditional expectation:

$$\hat{\mathbf{y}}_*[k] = E \left\{ \mathbf{Y}[k] \mid \mathbf{U}[k] = \mathbf{u}[k], \mathbf{Y}[k-1] = \mathbf{y}[k-1] \right\}, \quad (3)$$

which is, in the least square sense, the best prediction for the output given its previous values.<sup>1</sup>

Ideally the model predicted output  $\hat{\mathbf{y}}[k]$  should be as close as possible to the optimal one  $\hat{\mathbf{y}}_*[k]$ . This could be accomplished by minimizing the *ideal* cost function:

$$V_*(\boldsymbol{\theta}) = \frac{1}{N} \sum_{k=1}^N \|\hat{\mathbf{y}}_*[k] - \hat{\mathbf{y}}[k]\|^2, \quad (4)$$

which, however, is not available for optimization. Nevertheless, under some regularity conditions, it has been proved that [8]:

$$\arg \min V \rightarrow \arg \min V_* \text{ with probability 1 as } N \rightarrow \infty \quad (5)$$

that is, the minimizers of the cost function (1) asymptotically converge to the minimizers of (4). Also, this convergence is uniform.

When  $V_*$  has a single point as its minimizer, this result implies, under additional regularity conditions on the

<sup>1</sup> This prediction provides the smallest squared conditional expected error between the predicted and observed values:

$$\hat{\mathbf{y}}_*[k] = \arg_{\hat{\mathbf{y}}} \min E \left\{ \|\mathbf{Y}[k] - \hat{\mathbf{y}}\|^2 \mid \mathbf{U}[k], \mathbf{Y}[k-1] \right\}.$$

input, that prediction error methods yield consistent estimators<sup>2</sup> [8]. Additionally, in [33] it is shown that for a single point global solution the estimator has a normal asymptotic distribution.

### 2.4 Examples

Commonly used prediction error methods fit into the previous framework, as shown below for (a) nonlinear ARX models, which are models obtained by minimizing the one-step-ahead prediction of a difference equation; (b) nonlinear ARMAX<sup>3</sup> models, which add noise terms to the estimation; and, (c) output error models, which minimize the free-run simulation error of a difference equation. These three methods arise from the following different hypotheses about how the noise affects the data-generating process, respectively:

- a)  $\mathbf{Y}[k] = \mathbf{f}^*(\mathbf{Y}[k-1], \mathbf{U}[k]; \boldsymbol{\theta}^*) + \mathbf{V}[k]$
- b)  $\mathbf{Y}[k] = \mathbf{f}^*(\mathbf{Y}[k-1], \mathbf{U}[k], \mathbf{V}[k-1], \dots, \mathbf{V}[k-n_v]; \boldsymbol{\theta}^*) + \mathbf{V}[k]$
- c)  $\begin{cases} \tilde{\mathbf{Y}}[k] = \mathbf{f}^*(\tilde{\mathbf{Y}}[k-1], \dots, \tilde{\mathbf{Y}}[k-n_y], \mathbf{U}[k]; \boldsymbol{\theta}^*) \\ \mathbf{Y}[k] = \tilde{\mathbf{Y}}[k] + \mathbf{V}[k]. \end{cases}$

In (a), the output  $\mathbf{Y}$  is disturbed by the presence of a white random process  $\mathbf{V}$ . In (b), we have a more general noise structure, for which past values of  $\mathbf{V}$  can interfere in the current output. In both cases, this error, called *equation error*, changes the system trajectory. In (c), the error only affects the measured values and not the system trajectory and is called *output error*.

The *optimal predictors*, defined as in (3), follow from the data-generating processes and have the following closed-form expressions:

- a)  $\hat{\mathbf{y}}_*[k] = \mathbf{f}^*(\mathbf{y}[k-1], \mathbf{u}[k]; \boldsymbol{\theta}^*)$ .
- b)  $\begin{cases} \mathbf{v}[k] = \mathbf{y}[k] - \mathbf{f}^*(\mathbf{y}[k-1], \mathbf{u}[k], \mathbf{v}[k-1], \dots, \mathbf{v}[k-n_v]; \boldsymbol{\theta}^*) \\ \hat{\mathbf{y}}_*[k] = \mathbf{f}^*(\mathbf{y}[k-1], \mathbf{u}[k], \mathbf{v}[k-1], \dots, \mathbf{v}[k-n_v]; \boldsymbol{\theta}^*) \end{cases}$
- c)  $\begin{cases} \tilde{\mathbf{y}}[k] = \mathbf{f}^*(\tilde{\mathbf{y}}[k-1], \dots, \tilde{\mathbf{y}}[k-n_y], \mathbf{u}[k]; \boldsymbol{\theta}^*) \\ \hat{\mathbf{y}}_*[k] = \tilde{\mathbf{y}}[k], \end{cases}$

and, we choose the *prediction models* to be, respectively:

- a)  $\hat{\mathbf{y}}[k] = \mathbf{f}(\mathbf{y}[k-1], \mathbf{u}[k]; \boldsymbol{\theta})$ .
- b)  $\begin{cases} \mathbf{v}[k] = \mathbf{y}[k] - \mathbf{f}(\mathbf{y}[k-1], \mathbf{u}[k], \mathbf{v}[k-1], \dots, \mathbf{v}[k-n_v]; \boldsymbol{\theta}) \\ \hat{\mathbf{y}}[k] = \mathbf{f}(\mathbf{y}[k-1], \mathbf{u}[k], \mathbf{v}[k-1], \dots, \mathbf{v}[k-n_v]; \boldsymbol{\theta}) \end{cases}$
- c)  $\begin{cases} \tilde{\mathbf{y}}[k] = \mathbf{f}(\tilde{\mathbf{y}}[k-1], \dots, \tilde{\mathbf{y}}[k-n_y], \mathbf{u}[k]; \boldsymbol{\theta}) \\ \hat{\mathbf{y}}[k] = \tilde{\mathbf{y}}[k]. \end{cases}$

The reason for choosing these prediction models is that, under the right model structure (i.e.  $\mathbf{f} = \mathbf{f}^*$ ) the *true* parameter  $\boldsymbol{\theta}^*$  will be one of the minimizers of  $V_*$ . Hence, by (5), the parameters estimated using the prediction

<sup>2</sup> An estimator is consistent if the estimated parameters converge toward the *true* parameters as  $N \rightarrow \infty$ .

<sup>3</sup> *Autoregressive moving average with exogenous input* (ARMAX) model.

error method framework will be, for a sufficiently large  $N$  and ideal optimization process, arbitrarily close to  $\theta^*$  or to a solution with equivalent performance. Choosing the right model structure might be impossible in a practical application, nevertheless there exist families of universal approximator functions (e.g. neural networks and polynomials) for which the distance  $\|\mathbf{f} - \mathbf{f}^*\|$  might be made arbitrarily small within a compact set. So, this condition is not so restrictive as it might sound at first. We should also highlight that there has been a slight abuse of notation when defining the *prediction model*, while for the optimal predictor case  $\mathbf{v}[k]$  and  $\bar{\mathbf{y}}[k]$  can be interpreted as realizations of the corresponding random variables, for the prediction model with  $\theta \neq \theta^*$  there are no such guarantees, and these variables should be interpreted only as auxiliary variables.

It is interesting to see how, depending on how the noise affects the system, estimating a difference equation might, for property (5) to hold, require different *prediction models*. Nevertheless, these three prediction models can all be written as in equation (2). For (a), the model has an empty state vector; for (b), the state vector contains previous estimates of the noise  $\mathbf{x}[k] = [\mathbf{v}^T[k-1], \dots, \mathbf{v}^T[k-n_v]]^T$ ; and, for (c), the output model contains estimates of the noise-free output  $\mathbf{x}[k] = [\bar{\mathbf{y}}[k]^T, \dots, \bar{\mathbf{y}}[k-n_y]]^T$ .

### 2.5 Initial conditions

In order for (5) to hold, the model needs to be simulated starting with appropriate initial conditions  $\mathbf{x}_0$ . Since the true initial condition  $\mathbf{x}_0^*$  is unknown, there are two possible approaches when estimating the parameters.

The first approach is to fix  $\mathbf{x}_0$ , for some  $\mathbf{x}_0 \approx \mathbf{x}_0^*$ , and minimize the cost function (1). This approach is based on the idea that, for an asymptotically stable system, the influence of the initial conditions on the output decreases with time and, hence, even if  $\mathbf{x}_0 \neq \mathbf{x}_0^*$  we can still obtain a good estimate of the parameters. In this case the first samples may be discarded, to make sure the transient errors are not too large. For situation (b) in Section 2.4, an appropriate choice of initial values would be  $\mathbf{v}[k] = \mathbf{0}$ ,  $k = 1, \dots, n_v$  and, for situation (c),  $\bar{\mathbf{y}}[k] = \mathbf{y}[k]$ ,  $k = 1, \dots, n_y$ .

The second approach consists of including  $\mathbf{x}_0$  in the optimization problem, so it converges to  $\mathbf{x}_0^*$  and improves the quality of the parameter estimates. The optimization problem to be solved in this case is to minimize  $V$  with both  $\theta$  and  $\mathbf{x}_0$  as optimization variables:

$$\min_{\theta, \mathbf{x}_0} V. \quad (6)$$

## 3 Smoothness of prediction error methods

The theorem below relates the Lipschitz constant of  $V$ , and its gradient (i.e.  $\beta$ -smoothness), to the simulation length  $N$ . The Lipschitz constant of the cost function and the  $\beta$ -smoothness both play a crucial role in optimization [34]. Lower values imply that local (Taylor) expansions of the cost function are more predictive of the cost function, and that optimization algorithms can still converge while taking larger steps. It also gives an upper bound on how distinct in performance two close local minima may be.

**Theorem 1** *Let  $\mathbf{h}(\mathbf{x}, \mathbf{z}; \theta)$  and  $\mathbf{g}(\mathbf{x}, \mathbf{z}; \theta)$  in (2) be Lipschitz in  $(\mathbf{x}, \theta)$  with constants  $L_h$  and  $L_g$  on a compact and convex set  $\Omega = (\Omega_{\mathbf{x}}, \Omega_{\mathbf{z}}, \Omega_{\theta})$ . With  $\{\mathbf{z}[k]\}_{k=1}^N \subseteq \Omega_{\mathbf{z}}$  and  $(\Omega_{\mathbf{x}}, \Omega_{\theta}) \subseteq \mathbb{R}^{N_x} \times \mathbb{R}^{N_{\theta}}$ . If there exist at least one choice of  $(\mathbf{x}_0, \theta)$  for which there is an invariant set contained in  $\Omega$ , then, for trajectories and parameters confined within  $\Omega$ :*

- (1) *The cost function  $V$  defined in (1) is Lipschitz with constant:*<sup>4</sup>

$$L_V = \begin{cases} \mathcal{O}(L_h^{2N}) & \text{if } L_h > 1, \\ \mathcal{O}(N) & \text{if } L_h = 1, \\ \mathcal{O}(1) & \text{if } L_h < 1. \end{cases} \quad (7)$$

- (2) *If the Jacobian matrices of  $\mathbf{h}$  and  $\mathbf{g}$  are also Lipschitz with respect to  $(\mathbf{x}, \theta)$  on  $\Omega$ , then the gradient of the cost function  $\nabla V$  is also Lipschitz with constant:*

$$L'_V = \begin{cases} \mathcal{O}(L_h^{3N}) & \text{if } L_h > 1, \\ \mathcal{O}(N^3) & \text{if } L_h = 1, \\ \mathcal{O}(1) & \text{if } L_h < 1. \end{cases} \quad (8)$$

**PROOF.** See Appendix B.

For contractive models<sup>5</sup>, under certain regular conditions, we have  $L_h < 1$  and, accordingly to the above theorem, both the Lipschitz constant and the  $\beta$ -smoothness of the cost function can be bounded by a constant that, asymptotically, does not depend on the simulation length. All contractive systems have a unique fixed point inside the contractive region, and all trajectories converge to such a fixed point [35, Theorem 9.23]. Systems with richer nonlinear dynamic behaviours, such

<sup>4</sup> Where  $\mathcal{O}$  denotes the big O notation. It should be read as:  $L(N) = \mathcal{O}(g(N))$  if and only if there exists positive integers  $M$  and  $N_0$  such that  $|L(N)| \leq M g(N)$  for all  $N \geq N_0$ .

<sup>5</sup> We say a dynamical system  $\mathbf{x}[k+1] = \mathbf{h}(\mathbf{x}[k])$  is *contractive* if, for all  $\mathbf{x}$  and  $\mathbf{w}$ , it satisfies  $\|\mathbf{h}(\mathbf{x}) - \mathbf{h}(\mathbf{w})\| < L \|\mathbf{x} - \mathbf{w}\|$ , for  $L < 1$ .

as limit cycles and chaotic attractors, and also unstable systems, are *non-contractive* and will always have  $L_h \geq 1$ . The Lipschitz constants and  $\beta$ -smoothness for these systems may, according to Theorem 1, blow up exponentially (or polynomially for some limit cases) with the maximum simulation length.

In a less formal way, for models that have infinitely long dependencies (i.e. are non-contractive) the distance between predicted and measured values might become progressively larger along the simulation length because errors will accumulate. This might yield very intricate objective functions in some parts of the parameter space making the optimization problem either very dependent on the initial point or very hard to optimize using non-linear programming methods.

## 4 Multiple shooting

In this section, we propose, in the context of prediction error methods, the application of a technique called *multiple shooting* for which the maximum simulation length is a design parameter. This enables solving problems that would be impossible or very hard to solve in the setting of Section 2, which will be called *single shooting*.

### 4.1 Method formulation

For the *multiple shooting* formulation, rather than simulating the prediction model (2) through the entire dataset from a single initial condition vector  $\mathbf{x}_0$ , the data is split into  $M$  intervals  $\{[m_i + 1, m_{i+1}] \mid i = 1, \dots, M\}$ ,  $0 = m_1 < m_2 < \dots < m_M < m_{M+1} = N$ , each one with its own set of initial conditions  $\mathbf{x}_0^i \in \mathbb{R}^{N_x}$ . The  $i$ -th vector of initial conditions  $\mathbf{x}_0^i$  is used in the computation of the prediction  $\hat{\mathbf{y}}^i[k]$  in the interval  $m_i + 1 \leq k \leq m_{i+1}$ :

$$\begin{aligned} \mathbf{x}^i[k] &= \mathbf{h}(\mathbf{x}^i[k-1], \mathbf{z}[k]; \boldsymbol{\theta}), \text{ for } \mathbf{x}^i[m_i] = \mathbf{x}_0^i, \\ \hat{\mathbf{y}}^i[k] &= \mathbf{g}(\mathbf{x}^i[k], \mathbf{z}[k]; \boldsymbol{\theta}). \end{aligned} \quad (9)$$

Since the length of the simulation is limited to the smaller interval  $[m_i + 1, m_{i+1}]$ , the trajectory is less likely to strongly diverge and this typically helps the optimization procedure by making the objective function *smoother*.

Let,  $\Delta m_i = m_{i+1} - m_i$ , we define:

$$V_i = \frac{1}{\Delta m_i} \sum_{k=m_i+1}^{m_{i+1}} \|\mathbf{y}[k] - \hat{\mathbf{y}}^i[k]\|^2, \quad i = 1, \dots, M \quad (10)$$

to be the cost function associated with the  $i$ -th interval. Where the prediction  $\hat{\mathbf{y}}^i[k]$  depends upon  $\boldsymbol{\theta}$  and  $\mathbf{x}_0^i$ , according to (2). The *multiple shooting* formulation has as

objective function:

$$V^M = \sum_{i=1}^M \frac{\Delta m_i}{N} V_i. \quad (11)$$

This objective function includes states  $\mathbf{x}_0^1, \dots, \mathbf{x}_0^M$  as free variables in the optimization. Hence, rather than reinforcing the cohesion of the states  $\mathbf{x}[k]$  by defining them through a recurrence relation that casts a dependency of  $\mathbf{x}[k]$  all the way back to the initial condition  $\mathbf{x}_0$ , as in the *single shooting* formulation, the cohesion between subsequent states is achieved through optimization constraints, resulting in the following problem:

$$\begin{aligned} \min_{\boldsymbol{\theta}, \mathbf{x}_0^1, \dots, \mathbf{x}_0^M} \quad & V^M, \\ \text{subject to: } \quad & \mathbf{x}^{i-1}[m_i] = \mathbf{x}_0^i, \\ & \text{for } i = 2, 3, \dots, M. \end{aligned} \quad (12)$$

The next theorem gives the equivalence between (6) and (11) and Fig. 1 gives some insight into how the constraints in the *multiple shooting* formulation are used to imitate a single simulation throughout the entire dataset.

**Theorem 2** *If  $\mathbf{x}^{i-1}[m_i] = \mathbf{x}_0^i$ , for  $i = 2, 3, \dots, M$  and  $\mathbf{x}_0^1 = \mathbf{x}_0$ , then  $V = V^M$ .*

**PROOF.** Let us call  $\mathbf{x}[k]$ ,  $\hat{\mathbf{y}}[k]$  and  $\mathbf{x}^i[k]$ ,  $\hat{\mathbf{y}}^i[k]$  the states and predictions, respectively, in the single shooting simulation and in the  $i$ -th multiple shooting interval. For a fixed  $i$ , if  $\mathbf{x}[m_i] = \mathbf{x}_0^i$  then  $\mathbf{x}[k] = \mathbf{x}^i[k]$  for all  $k \in [m_i + 1, m_{i+1}]$ . Hence, inside this same interval  $\hat{\mathbf{y}}[k] = \hat{\mathbf{y}}^i[k]$ . Applying this for every  $i$  it follows from the respective definitions that:  $V = \sum_{i=1}^M \frac{\Delta m_i}{N} V_i = V^M$ .

**Corollary 3** *The pair  $(\boldsymbol{\theta}^*, \mathbf{x}_0^*)$  is a global solution of (6) if and only if there exist  $(\mathbf{x}_0^1, \dots, \mathbf{x}_0^M)$  such that  $(\boldsymbol{\theta}^*, \mathbf{x}_0^1, \mathbf{x}_0^2, \dots, \mathbf{x}_0^M)$  is a global solution of the optimization problem (12).*

The cost function that arises in the multiple shooting formulation has some nice properties that will be investigated in the next section. Besides that, another advantage of multiple shooting is that it is more amenable to parallelization, since, each cost function  $V_i$  and the respective derivatives can be computed independently and, possibly, in parallel. Finally, multiple shooting can be understood as a generalization of the single shooting case. That is because, if  $M = 1$  and  $\Delta m_1 = N$ , multiple and single shooting result in the same optimization problem.

### 4.2 Properties of the objective function

The next theorem relates the Lipschitzness and  $\beta$ -smoothness of the cost function  $V^M$  with that of its

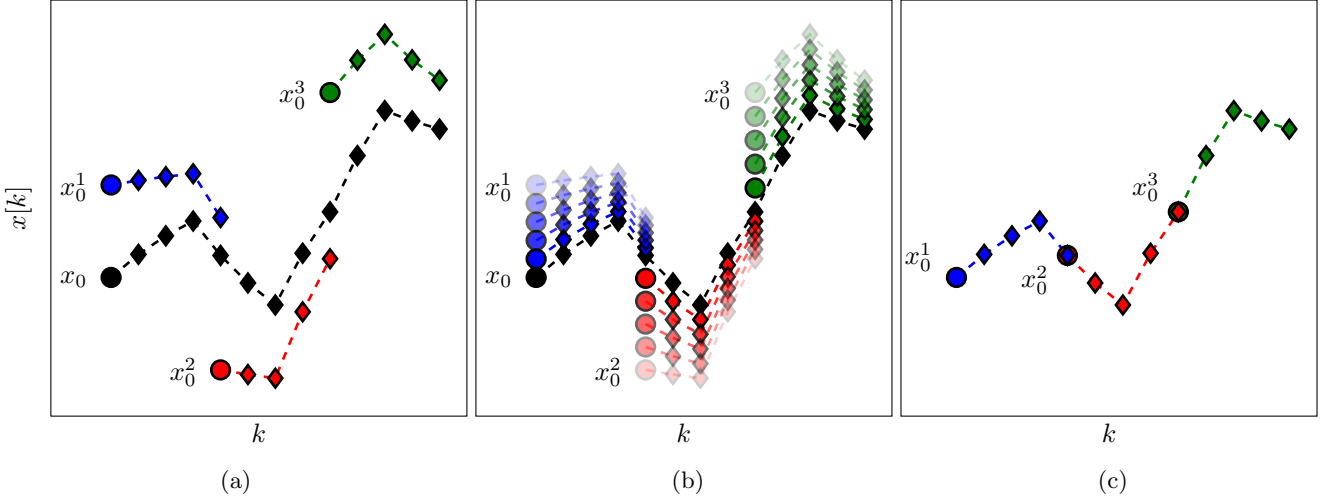


Fig. 1. Comparison between single shooting and multiple shooting in a unidimensional example ( $N^x = 1$ ). In **black** we present the simulation of the dynamic system through the entire window length using the single initial condition  $x_0$  (represented by  $\bullet$ ). The simulated values are represented by  $\blacklozenge$ . Dividing the window length into three sub-intervals and simulating the system in each of these, for initial conditions  $x_0^1$ ,  $x_0^2$ , and  $x_0^3$ , results in the three different simulations represented by  $\bluelozenge$ ,  $\redlozenge$  and  $\greenlozenge$ , respectively. In (a), the end of one simulation does not coincide with the beginning of the next one ( $x^{i-1}[m_i] \neq x_0^i$ ). In (b), we show what happens as  $\|x^{i-1}[m_i] - x_0^i\| \rightarrow 0$ . And, in (c), we show that, when  $x^{i-1}[m_i] = x_0^i$ , the concatenation of these short simulations is equivalent to a single one carried out over the entire window length.

components  $V_i$ .

**Theorem 4** Define  $V^M$  as in (11), if each component  $V_i$  is Lipschitz continuous with constant  $L_{V_i}$ , then  $V^M$  is also Lipschitz with constant equal to or smaller than  $L_{V^M} = \max(L_{V_1}, \dots, L_{V_M})$ . Additionally, if the gradient of each component  $\nabla V_i$  is Lipschitz continuous with constant  $L'_{V_i}$ , then  $\nabla V^M$  is also Lipschitz with constant equal to or smaller than  $L'_{V^M} = \max(L'_{V_1}, \dots, L'_{V_M})$ .

**PROOF.** For  $\theta_{\text{ext}} = (\theta, x_0^1, \dots, x_0^M)$  and  $\phi_{\text{ext}} = (\phi, w_0^1, \dots, w_0^M)$  we have that:

$$\begin{aligned} |V^M(\theta_{\text{ext}}) - V^M(\phi_{\text{ext}})| &\leq \\ &\sum_{i=1}^M \frac{\Delta m_i}{N} |V_i(\theta, x_0^i) - V_i(\phi, w_0^i)| \leq \\ &\sum_{i=1}^M \frac{\Delta m_i}{N} L_{V_i} \|\theta, x_0^i\|^T - \|\phi, w_0^i\|^T\| \leq \\ &L_{V^M} \|\theta_{\text{ext}} - \phi_{\text{ext}}\|, \end{aligned}$$

where  $L_{V^M} = \max(L_{V_1}, \dots, L_{V_M})$ . And similarly,  $L'_{V^M} = \max(L'_{V_1}, \dots, L'_{V_M})$ , which yields the second result.

Putting together Theorems 1 and 4 we have that  $L_{V^M}$  and  $L'_{V^M}$  depend asymptotically on  $\Delta m_{\text{max}} =$

$\max_{1 \leq i \leq M} \Delta m_i$  and not on  $N$ . For instance, if  $L_h > 1$ :

$$L_{V^M} = \mathcal{O}(L_h^{2\Delta m_{\text{max}}}); \quad L'_{V^M} = \mathcal{O}(L_h^{3\Delta m_{\text{max}}}). \quad (13)$$

Since  $\Delta m_{\text{max}}$  is a design parameter, we can actually have some control over the Lipschitzness and  $\beta$ -smoothness of the objective function for models where  $L_h \geq 1$ . Hence multiple shooting might help considerably when estimating parameters of non-contractive models ( $L_h \geq 1$ ).

### 4.3 Comparison with other methods

Multiple-shooting is presented here as a possible way of limiting the maximum simulation length  $\Delta m_{\text{max}}$ . A method that appears in the system identification literature that also has a similar effect is the minimization of the multi-step-ahead prediction error [36], [37], [38], [39], [40]. For those methods, the simulation is truncated by a fixed number  $K$  of steps backwards. That is, given  $k$ , we define an auxiliary variable  $\tilde{x}_k[i]$  and use the state equations:  $\tilde{x}_k[i] = \mathbf{h}(\tilde{x}_k[k-1], \mathbf{z}[k]; \theta)$  to simulate the evolution of this auxiliary state variable for  $i = k-K, \dots, k$ , starting from a fixed initial condition  $\tilde{x}_k[k-K] = \tilde{x}_{0,k}$ . The prediction is then computed using  $\hat{\mathbf{y}}[k] = \mathbf{g}(\tilde{x}_k[k], \mathbf{z}[k]; \theta)$ . The parameters are obtained by minimizing a cost function similar to (1).

The use of multi-step-ahead prediction is equivalent to the original single shooting formulation only if  $K = N$ . Hence, it imposes a trade-off between: i) the benefits of using a recursive model (such as better properties for



non-white process noise) for larger values of  $K$ ; and, ii) the benefits of having a smaller simulation length (such as smother cost function for non-contractive models, by Theorem 1) for smaller values of  $K$ . Multiple shooting, on the other hand, has an exact equivalence with the original single shooting problem regardless of the simulation length (see Theorem 2 and Corollary 3), so both desirable characteristics are obtained at once.

The computational cost for computing  $V$  and its derivatives is  $K$  times greater for multi-step-ahead than for the multiple shooting method, because of the need to propagate the auxiliary variables  $\tilde{\mathbf{x}}_k$ . On the other hand, multi-step-ahead prediction yields an unconstrained problem, rather than a constrained one, for which more efficient solvers might be available. Also, it does not include initial state variables in the optimization problem, what results in a lower dimensional problem. While the larger number of parameters in the multiple-shooting does not increase the computational cost so much, because of the underlying sparse structure of the problem, it does require a careful implementation with smart use of those properties.

The limitations of such methods in the fully nonlinear setting presented in this paper might be avoided in some special cases. Currently, to the best of our knowledge, multi-step-ahead prediction has been studied primarily in a linear model setting [36], [37], [38], [39], [40], for which these methods might result in convex optimization problems. They are most popular for system identification in model predictive control problems, for which the multi-step-ahead prediction usually fits well into the moving horizon framework and allows for more efficient implementations [37], [39], [40].

## 5 Implementation and numerical examples

The equality constraint problem (11) from the multiple shooting formulation is solved using an implementation of the sequential quadratic programming solver originally described in [41]. The procedure used for computing the derivatives is explained in Appendix A. The code for reproducing the examples is available in the GitHub repository: [github.com/antonior92/MultipleShootingPEM.jl](https://github.com/antonior92/MultipleShootingPEM.jl).

### 5.1 Example 1: output error model for chaotic system

This example illustrates how multiple shooting makes prediction error methods more robust against the choice of initial conditions for the optimization. A dataset with  $N = 200$  samples is generated using the logistic map [42]:

$$y[k] = \theta y[k-1](1 - y[k-1]), \quad (14)$$

with  $\theta = 3.78$ . From the generated dataset we try to estimate an *output error* model with the same structure.

Figure 2 (a) illustrates the objective function for the *single shooting* case. The model that is being fitted to the data presents a chaotic behavior for  $\theta \in [3.57, 4]$ , which justifies the very intricate objective function in this region. For chaotic systems, small variations in the parameters may cause large variations in the system trajectory and, hence, abrupt changes in the *free-run simulation error*. This is the reason why the estimation of an output error model has many local solutions in this problem.

The solutions found by the solver, for different initial guesses, are also displayed in Figure 2 (a). Notice that the solver fails to find the true solution because it always gets trapped at a local stationary point near its initial guess. Even in the noise-free situation we are considering, the identification procedure is made very challenging by the chaotic nature of the system, that, for a long enough simulation, yields large trajectory differences even for small parameter variations.

Multiple shooting makes the problem easier by limiting the total simulation length. Figures 2 (b), (c) and (d) display the objective function and the solutions found by the solver starting from different initial guesses. Each figure displays the result for a different choice of  $\Delta m_{\max}$ : For (b) the maximum simulation length is  $\Delta m_{\max} = 10$ ; for (c),  $\Delta m_{\max} = 5$ ; and, for (d),  $\Delta m_{\max} = 2$ .

The identification procedure becomes easier as  $\Delta m_{\max}$  is made smaller. For Figures (b) and (c) the solver converges to the true parameter for some initial guesses but, also, to undesirable local solutions for other initializations. For Figure (d) the solver converges to the true solution regardless of the initial guess.

For the multiple shooting case, besides  $\theta$ , the initial conditions are also optimization parameters. To help with the visualization of this multidimensional problem, Figures 2 (b), (c) and (d) display the main curve corresponding to the objective function for the true initial conditions and faded lines corresponding to the objective function for perturbed initial conditions. Another consequence of the problem having more parameters than displayed in the figure is that the cost function found by the solver does not need to lie on any of the objective function curves displayed in the figure, since it may have a different set of initial conditions  $\mathbf{x}_0^i$ .

Table 1 gives the number of function evaluations and the running time for the four situations displayed in Figure 2. The convergence happens within just a few iterations for  $\Delta m_{\max} = N$  (single shooting) because any initial point is probably very close to some optimal *local* solution. As we reduce  $\Delta m_{\max}$  the objective function becomes less intricate and this is reflected in the convergence of the solver. For  $\Delta m_{\max} = 10$  the solver takes much longer to converge. We believe this happens because the local solution is not so close in the parameter space to the initial guess anymore. As we further decrease  $\Delta m_{\max}$ ,

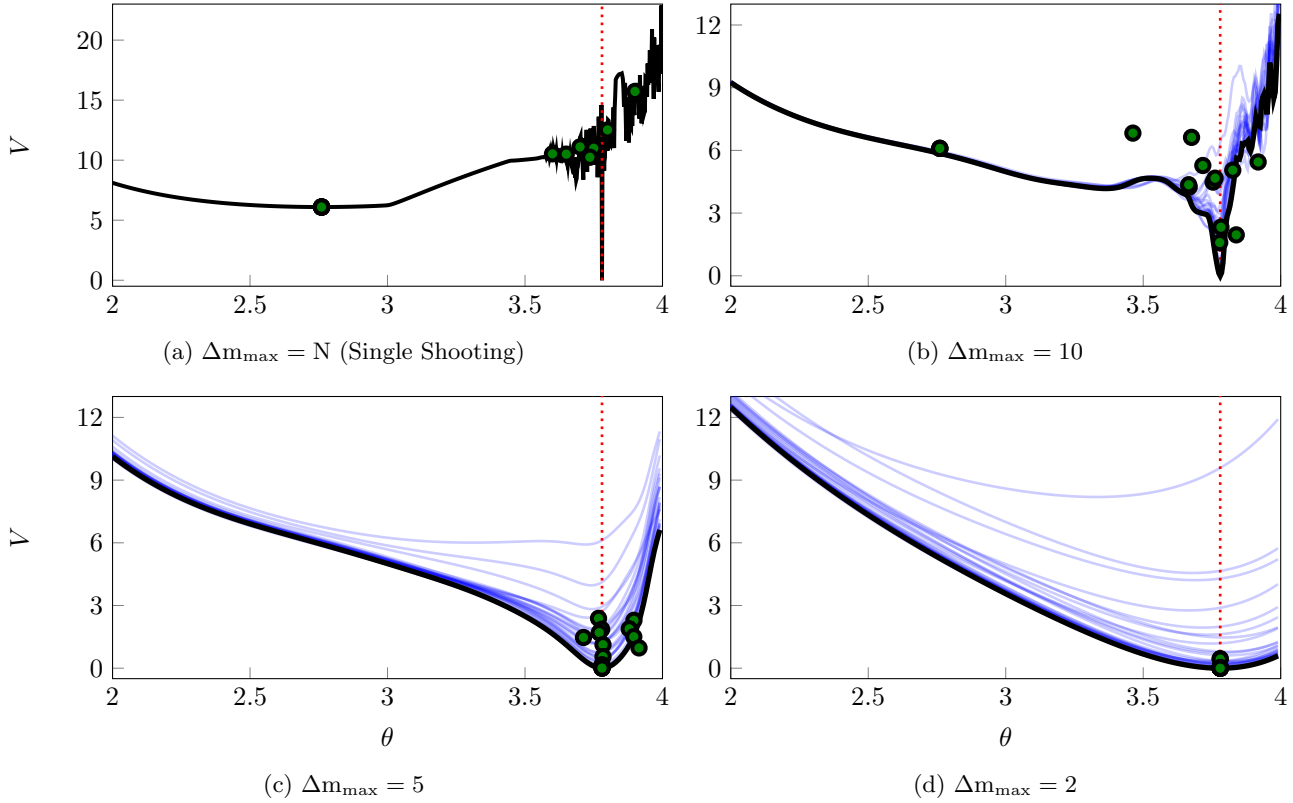


Fig. 2. **(Example 1)** *Cost function* of the optimization problem for  $\mathbf{x}_0^i$  fixed in its true values (in black) and for disturbed versions of these initial conditions (in blue). We present the result for four values of  $\Delta m_{\max}$ , and omit disturbed initial condition objective functions for the single shooting case ( $\Delta m_{\max} = N$ ) to make it easier to visualize. The green circles,  $\bullet$ , indicate the pair  $(\theta, V)$  corresponding to a solution found by the solver. There are 15 circles in each figure (some of them overlapping), the circles correspond to solutions for different initial guesses. As initial guesses we picked values of  $\theta$  uniformly spaced between 3.2 and 3.9, with  $\mathbf{x}_0^i$  picked from randomly disturbed versions of the true initial conditions (which are known because we generated the data ourselves). The true value  $\theta = 3.78$  is indicated by the dotted red vertical line.

however, the convergence becomes faster, because it is dealing with, what we believe to be, a smoother problem that can be more accurately approximated by low order approximations.

Table 1

Number of function evaluations and total running time to convergence for different values of  $\Delta m_{\max}$ . We give, the minimum, maximum and median among 15 runs for the situations presented in Figure 2. (\*) The number of iterations is limited to 1000 and the solver is interrupted when this number is reached.

$\Delta m_{\max}$	function evaluations			run time (s)		
	min	median	max	min	median	max
$N$	1	15	23	0.01	0.2	1.1
10	43	1000*	1000*	0.7	24.7	27.3
5	29	115	645	1.0	2.9	26.9
2	21	50	65	1.7	2.9	3.8

## 5.2 Example 2: neural network for modeling pilot plant

This example uses data from the level process station described in Example 1 from [18]. As in the original paper, we use a neural network to model the water column height as a function of the voltage applied to a control valve that modulates the water flow. We compare three different training methods: i) minimizing the one-step-ahead prediction error (NN ARX) ii) minimizing the free-run simulation error using single shooting method (NN OE - SS); and, iii) minimizing the free-run simulation error using multiple shooting method (NN OE - MS).

The neural network (NN) training depends on the weight initialization, hence the performance of the neural network can be regarded as a random variable and is displayed in Figure 3, which compares the empirical cumulative distribution of the *mean square error* (MSE) over the validation dataset for the three methods. A linear ARX model ( $n_y = 1$  and  $n_u = 1$ ) was trained and tested under the same conditions to serve as the baseline. Methods (i) and (ii) and the linear ARX baseline



were described in [18]. Method (iii) is introduced here.

The cumulative distribution function gives, for each  $x$ -axis value, the probability of the method to yield a validation MSE smaller or equal to this value. It was estimated from 100 realizations of the neural network training procedure. Figure 3 shows that for more than 90% of the realizations, estimating the parameters by minimizing the free-run simulation (NN OE) offers significant advantages over the minimization of the one-step-ahead error (NN ARX). When using a standard single shooting formulation, however, it also makes the parameter estimation procedure more sensitive to the initial conditions, with the algorithm yielding some really bad results for some initial choices [18]. This results in a long-tailed distribution for the MSE (Fig. 3). More precisely, in 10 out of 100 realizations the NN OE - SS model yields a performance that is inferior to the linear ARX baseline, some of the realizations worse than the linear baseline by a factor of 100. The performance of the NN OE - SS and NN OE - MS is very similar for 90% of the realizations, the tail of the distribution, however, is very different, with the multiple shooting procedure rarely producing very bad results. In order to highlight the differences, results where NN OE - SS and NN OE - MS are worse than the baseline are presented, respectively, as blue and red circles in Fig. 3.

This example illustrates how the use of multiple shooting alleviates the problem of high sensitivity to initial conditions, making it possible to estimate output error models with extra robustness against variations of the initial conditions and lower probability of getting trapped at local minima with very bad performance.

This example also shows the limitations of the multiple shooting formulation. The training time for NN OE - MS model is 282 seconds, for NN OE - SS model is 3.9 seconds, and for NN ARX model is 3.3 seconds. This means that the single shooting parameter estimation could be repeated, roughly, 70 times for each multiple shooting run. Hence solving the single shooting problem several times and choosing the best result would also avoid very bad solutions and could, still, be computationally less expensive than solving the multiple shooting problem. The longer training time is due to two factors: i) per iteration the multiple shooting approach takes, roughly, 3.5 times more than the single shooting approach; and, ii) it takes, approximately, 20 times more iterations to converge. Both are consequences of the fact that a higher dimensional *constrained* optimization problem is being solved.

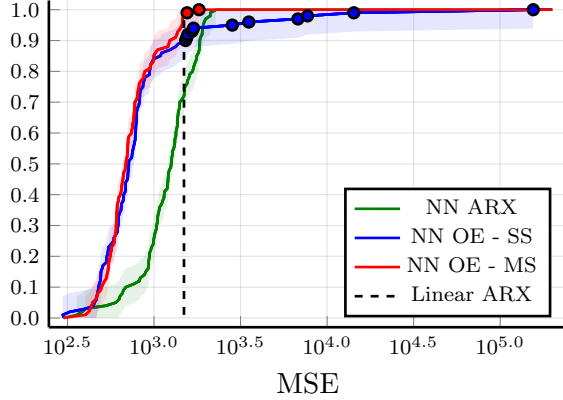


Fig. 3. **(Example 2)** Empirical cumulative distribution of the free-run simulation MSE over the validation dataset. The results obtained in [18] for an ARX neural network (NN ARX) and an (single shooting) output error neural network (NN OE - SS) are displayed together with the result obtained estimating the parameters using multiple shooting (NN OE - MS). A Linear ARX model is considered as a baseline and is displayed by the dashed line. The multiple shooting estimation uses  $\Delta m_{\max} = 3$  and the training is restricted to 2000 iterations of the optimization algorithm or until either the gradient or the step size drops below  $10^{-12}$ . The other models were estimated exactly as in [18]. All the neural network models have 10 nodes in the hidden layer,  $n_y = n_u = 1$  and were trained with the same training dataset. Each curve is the result of 100 realizations and, for each realization, the neural network initial weights  $w_{i,j}^{(n)}$  are drawn from a normal distribution with zero mean and standard deviation  $\sigma = (N_{s(n-1)})^{-0.5}$  and the bias terms  $\gamma_i^{(n)}$  are initialized with zeros [43]. Realizations of NN OE - SS and NN OE - MS that perform worse than the baseline are indicated respectively as blue, ●, and red circles, ●. Confidence intervals (95%) are displayed as shaded regions around the estimated cumulative distribution, these have been computed using the Dvoretzky-Kiefer-Wolfowitz inequality [44].

### 5.3 Example 3: pendulum and inverted pendulum

Consider the following discrete-time nonlinear system:

$$\begin{cases} x_1[k+1] = x_1[k] + \delta x_2[k] \\ x_2[k+1] = -\delta \frac{g}{l} \sin x_1[k] + (1 - \delta \frac{k_a}{m})x_2[k] + \delta \frac{1}{m}u[k] \\ y[k] = x_1[k] \end{cases} \quad (15)$$

which corresponds to a pendulum model, discretized using the Euler approximation  $\dot{x}(t) \approx \frac{x((k+1)\delta) - x(k\delta)}{\delta}$ . Where  $g$  is the gravity acceleration,  $m$  is the mass connected to the extremity of the pendulum,  $l$  is the length of the (massless) rod connecting the mass to the pivot point, and  $k_a$  is the linear friction constant. It has two states: the angle of the mass ( $x_1$ ) and the angular velocity ( $x_2$ ). The input  $u[k]$  is the force applied to the mass.

This system has multiple equilibrium points, namely,  $(x_1, x_2) = (\pm\pi i, 0)$  for  $i = 0, 1, 2, 3, \dots$ . The equilibrium

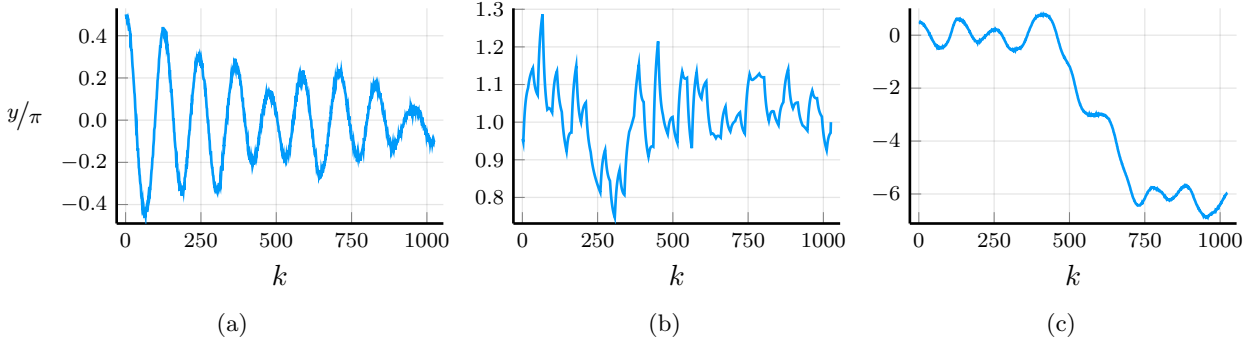


Fig. 4. **(Example 3)** Output signal  $y[k]$  for the three different datasets used for estimating the parameters. The dataset size is  $N = 1024$  samples. (a) The input applied in this case is a, zero mean, Gaussian random input with standard deviation  $\sigma_u = 10$ , each random value being hold for 20 samples. The input in this case is unable to drive the system away from the influence of the stable fixed point  $(0, 0)$ . (b) Same thing as (a) but with the larger standard deviation  $\sigma_u = 50$ , which is able to drive the pendulum to complete full rotations; and, (c) The input  $u[k]$  in this case is obtained by the control law:  $u[k] = 40\delta e[k-1] - 78.8\delta e[k-2] + 38.808\delta e[k-3] + 1.02u[k-1] - 0.02u[k-2]$ , where the error is the difference between the reference and the output:  $e[k] = r[k] - y[k]$ . The reference is  $r[k] = \pi + \Delta r[k]$  where  $\Delta r[k]$  is a, zero mean, Gaussian random input with standard deviation  $\sigma_r = 0.2$ , each random value being held for 20 samples. For (a) and (c) zero-mean Gaussian white noise with standard deviation  $\sigma_r = 0.03$  was added to the output.

points at  $(x_1, x_2) = (\pm 2\pi i, 0)$  are stable and the equilibrium points at  $(x_1, x_2) = (\pi \pm 2\pi i, 0)$  are unstable. For this system, with  $g = 9.8$ ,  $L = 0.3$ ,  $m = 3$ ,  $k_a = 2$  and  $\delta = 0.01$ , we define three different datasets: (a) A dataset for which small inputs are applied to the system, that stays under the influence of the stable point  $(x_1, x_2) = (0, 0)$  and  $y[k]$  stays, approximately, inside the range  $[-\frac{\pi}{2}, +\frac{\pi}{2}]$ ; (b) A dataset for which the system is maintained close to the unstable point  $(x_1, x_2) = (\pi, 0)$  by a linear controller; and, (c) A dataset for which the input is large enough to drive the pendulum to full rotations around its center. The output corresponding to those three situations are displayed in Figure 4.

Fixing  $m = 3$  and  $\delta = 0.01$  parameters  $\frac{g}{l}$  and  $k_a$  of an output error model with the structure presented in (15) were estimated from the data. A visualization of the cost function is presented in Figure 5 together with numerical solutions found by single shooting and multiple shooting formulation starting from different initial conditions.

For dataset (a), the single shooting formulation is able to recover the true parameters from data for most of the initial conditions. Some exceptions occur when initialized far away from the correct initial conditions. For datasets (b) and (c), for which the system needs, respectively, to operate close to the unstable dynamics or to account for the existence of multiple fixed points, the cost function is highly intricate, very non-convex and full of local minima. In this case, the optimization algorithm, even when initialized close to the local solution, fails to converge to reasonable solutions. This result is consistent with Theorem 1 and how the smoothness of the objective function degenerates (exponentially) on sets of the parameter space for which the prediction model is non-contractive, such as the trajectories close to the un-

stable fixed point of the system (15). The use of multiple shooting yields an objective function that looks similar to a paraboloid in the region of interest for the three cases, which suggests that local approximations might be valid over a large region. The solutions converge to the true parameter regardless of the initialization point in this formulation.

## 6 Conclusion and Future Work

The relevance of this paper lies in the very general setting for which the proposed methods and results hold. The major technical contribution is to show that for dynamic prediction models that are non-contractive (i.e. do not converge asymptotically to a single stable point) in the region of interest, the upper bound for the Lipschitz constant and the  $\beta$ -smoothness blows up exponentially with the simulation length, and this can make the optimization problem very hard to solve. This was illustrated with numerical examples with systems that are not contractive due to the presence of chaotic regions and non-stable equilibrium points. Because of these regimes, the objective function becomes very intricate in some regions of the parameter space and the optimization algorithm fails to find a good solution.

Multiple shooting makes the simulation length a design parameter and hence allows one to actually solve optimization problems that would be unfeasible in a single shooting setting. The price paid compared to single shooting methods is that a nonlinear constrained optimization problem should be solved instead of an unconstrained one. It also makes it harder to generalize to situations other than batch training, i.e. online training.

The study of other techniques, that allow to control

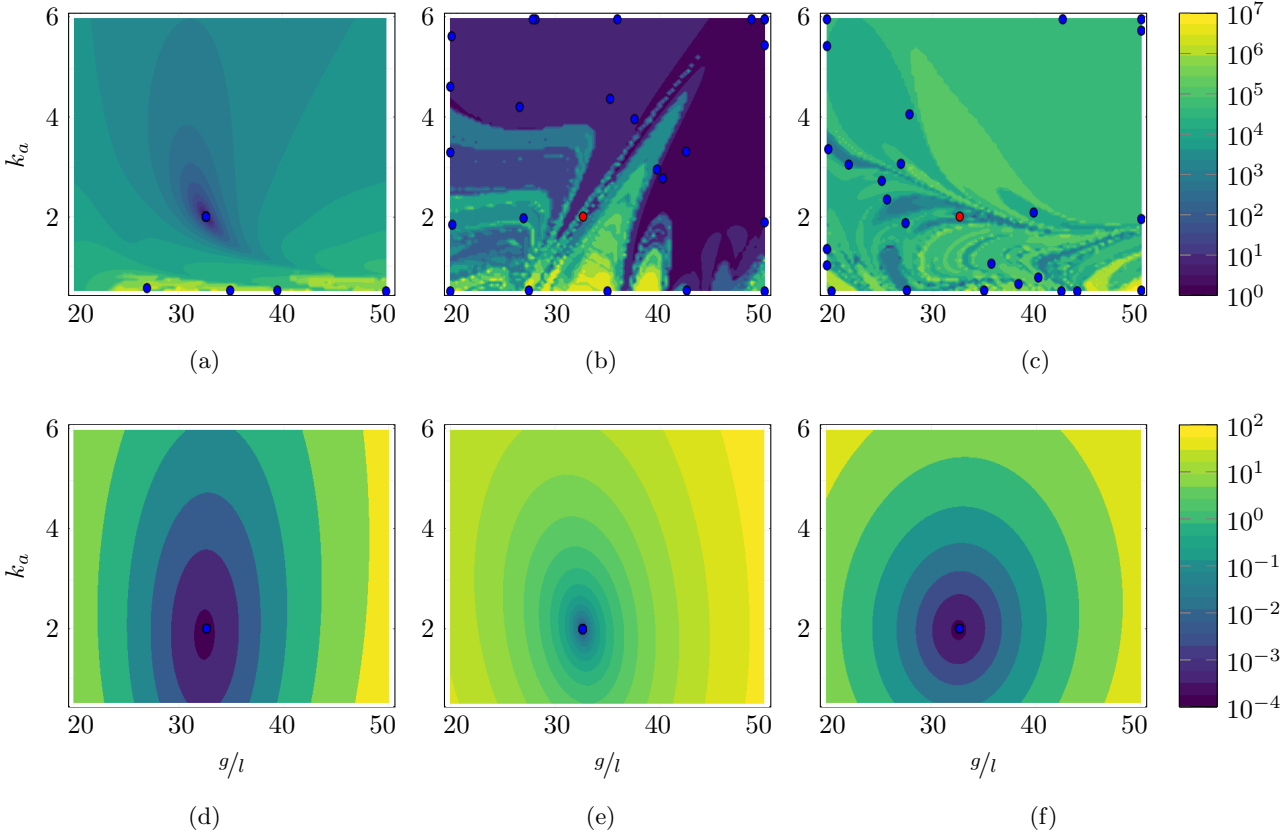


Fig. 5. **(Example 3)** *Contour plot of the cost function.* Figures (a), (b) and (c) correspond to the cost function  $V$  from single shooting simulation for the datasets (a), (b) and (c) generated as described in Fig. 4 caption; and, in (d), (e) and (f) the cost function for the same problems is displayed for the multiple shooting formulation with  $\Delta m_{\max} = 16$ . The true parameter is indicated by a red circle,  $\bullet$ , solutions found by the solver are indicated by blue circles,  $\bullet$ . There are 25 blue circles in each figure (some of them overlapping), each circle corresponds to the solution for a different initial guess. Some solutions are outside of the displayed region and the corresponding blue dots are displayed at the edge of the plot. Initial guesses were picked values of  $\theta$  uniformly spaced on a grid of points uniformly spaced in the rectangle  $[20, 50] \times [0.5, 6]$ . It is important to highlight that the plots show a two dimensional projection of a cost function that is defined on an extended parameter space that includes the initial conditions  $\mathbf{x}_0, i = 1, \dots, M$  as parameters, which were fixed to the true values when generating the contour plots.

the smoothness and Lipschitzness of the objective function in situations where the predictive model is non-contractive, are a natural continuation of this work. Theorem 1 makes it clear that both the maximum simulation length and the constant  $L_h$  are relevant design parameters. Multi-step-ahead prediction, described in Section 4.3 is another method that tries to introduce some control of the maximum simulation length. Another option, unexplored to the best of the authors knowledge, is to try to control  $L_h$ , this could be done by modifications in the state-transition. The amount of modification could be updated, adaptively, as the optimization algorithm approaches the final solution.

Results presented here might also be relevant for the community of recurrent neural networks, and might be helpful to understand in which situations exploding and vanishing gradients appear and how to handle them. We intend to explore these relations in future work. We

believe understanding the estimation of parameters for problems with recurrent structures in a fully nonlinear and non-convex setting is both very challenging and highly relevant for system identification and machine learning fields and that this paper is a step in the direction of a better understanding of this type of problems.

## Acknowledgements

This work has been supported by the Brazilian agencies *CAPES - Coordenacao de Aperfeiçoamento de Pessoal de Nível Superior* (Finance Code: 001), *CNPq - Conselho Nacional de Desenvolvimento Científico e Tecnológico* (contract number: 302079/2011-4, 200931/2018-0 and 142211/2018-4) and *FAPEMIG - Fundao de Amparo à Pesquisa do Estado de Minas Gerais* (contract number: TEC 1217/98), by the Swedish Research Council (VR) via the projects *NewLEADS - New Directions*

in *Learning Dynamical Systems* (contract number: 621-2016-06079) and *Learning flexible models for nonlinear dynamics* (contract number: 2017-03807), and by the Swedish Foundation for Strategic Research (SSF) via the project *ASSEMBLE* (contract number: RIT15-0012)

## References

- [1] L. Ljung, *System Identification*. Springer, 1998.
- [2] I. B. Tijani, R. Akmeliawati, A. Legowo, and A. Budiyo, "Nonlinear Identification of a Small Scale Unmanned Helicopter Using Optimized NARX Network with Multiobjective Differential Evolution," *Engineering Applications of Artificial Intelligence*, vol. 33, pp. 99–115, 2014.
- [3] B. O. S. Teixeira, W. S. Castro, A. F. Teixeira, and L. A. Aguirre, "Data-Driven Soft Sensor of Downhole Pressure for a Gas-Lift Oil Well," *Control Engineering Practice*, vol. 22, pp. 34–43, 2014.
- [4] R. J. Boynton, M. A. Balikhin, S. A. Billings, G. D. Reeves, N. Ganushkina, M. Gedalin, O. Amariutei, J. E. Borovsky, and S. N. Walker, "The Analysis of Electron Fluxes at Geosynchronous Orbit Employing a NARMAX Approach," *Journal of Geophysical Research: Space Physics*, vol. 118, no. 4, pp. 1500–1513, 2013.
- [5] S. M. Guzman, J. O. Paz, and M. L. M. Tagert, "The Use of NARX Neural Networks to Forecast Daily Groundwater Levels," *Water Resources Management*, vol. 31, no. 5, pp. 1591–1603, 2017.
- [6] F. da Costa Lopes, E. H. Watanabe, and L. G. B. Rolim, "A Control-Oriented Model of a PEM Fuel Cell Stack Based on NARX and NOE Neural Networks," *IEEE Transactions on Industrial Electronics*, vol. 62, no. 8, pp. 5155–5163, 2015.
- [7] J. R. Ayala Solares, H.-L. Wei, R. J. Boynton, S. N. Walker, and S. A. Billings, "Modeling and Prediction of Global Magnetic Disturbance in Near-Earth Space: A Case Study for Kp Index Using NARX Models," *Space Weather*, vol. 14, no. 10, pp. 899–916, 2016.
- [8] L. Ljung, "Convergence analysis of parametric identification methods," *IEEE Transactions on Automatic Control*, vol. 23, pp. 770–783, Oct. 1978.
- [9] K. Patan and J. Korbicz, "Nonlinear Model Predictive Control of a Boiler Unit: A Fault Tolerant Control Study," *International Journal of Applied Mathematics and Computer Science*, vol. 22, no. 1, pp. 225–237, 2012.
- [10] C. Zhang, K. Li, Z. Yang, L. Pei, and C. Zhu, "A new battery modelling method based on simulation error minimization," in *2014 IEEE PES General Meeting—Conference & Exposition*, 2014.
- [11] H. T. Su, T. J. McAvoy, and P. Werbos, "Long-Term Predictions of Chemical Processes Using Recurrent Neural Networks: A Parallel Training Approach," *Industrial & Engineering Chemistry Research*, vol. 31, no. 5, pp. 1338–1352, 1992.
- [12] H.-T. Su and T. J. McAvoy, "Neural Model Predictive Control of Nonlinear Chemical Processes," in *Intelligent Control, 1993., Proceedings of the 1993 IEEE International Symposium On*, pp. 358–363, IEEE, 1993.
- [13] L. Piroddi and W. Spinelli, "An Identification Algorithm for Polynomial NARX Models Based on Simulation Error Minimization," *International Journal of Control*, vol. 76, no. 17, pp. 1767–1781, 2003.
- [14] L. Piroddi, "Simulation Error Minimisation Methods for NARX Model Identification," *International Journal of Modelling, Identification and Control*, vol. 3, no. 4, pp. 392–403, 2008.
- [15] J. Paduart, L. Lauwers, J. Swevers, K. Smolders, J. Schoukens, and R. Pintelon, "Identification of nonlinear systems using Polynomial Nonlinear State Space models," *Automatica*, vol. 46, pp. 647–656, Apr. 2010.
- [16] M. Schoukens and K. Tiels, "Identification of block-oriented nonlinear systems starting from linear approximations: A survey," *Automatica*, vol. 85, pp. 272–292, Nov. 2017.
- [17] L. A. Aguirre, B. H. Barbosa, and A. P. Braga, "Prediction and simulation errors in parameter estimation for nonlinear systems," *Mechanical Systems and Signal Processing*, vol. 24, no. 8, pp. 2855–2867, 2010.
- [18] A. H. Ribeiro and L. A. Aguirre, "Parallel Training Considered Harmful?": Comparing series-parallel and parallel feedforward network training," *Neurocomputing*, vol. 316, pp. 222–231, Nov. 2018.
- [19] D. Eckhard, A. S. Bazanella, C. R. Rojas, and H. Hjalmarsson, "Cost function shaping of the output error criterion," *Automatica*, vol. 76, pp. 53–60, Feb. 2017.
- [20] H. Bock, "Recent Advances in Parameter Identification Problems for ODE," *Numerical Treatment of Inverse Problems in Differential and Integral Equations*, pp. 95–121, 1983.
- [21] E. Baake, M. Baake, H. Bock, and K. Briggs, "Fitting ordinary differential equations to chaotic data," *Physical Review A*, vol. 45, no. 8, p. 5524, 1992.
- [22] J. Timmer, H. Rust, W. Horbelt, and H. Voss, "Parametric, nonparametric and parametric modelling of a chaotic circuit time series," *Physics Letters A*, vol. 274, no. 3, pp. 123–134, 2000.
- [23] W. Horbelt, J. Timmer, M. Bünner, R. Meucci, and M. Ciofini, "Identifying physical properties of a CO2 LASER by dynamical modeling of measured time series," *Physical Review E*, vol. 64, no. 1, p. 016222, 2001.
- [24] M. Peifer and J. Timmer, "Parameter estimation in ordinary differential equations for biochemical processes using the method of multiple shooting," *IET Systems Biology*, vol. 1, no. 2, pp. 78–88, 2007.
- [25] K. D. Sarode, V. R. Kumar, and B. Kulkarni, "Embedded Multiple Shooting Methodology in a Genetic Algorithm Framework for Parameter Estimation and State Identification of Complex Systems," *Chemical Engineering Science*, vol. 134, pp. 605–618, 2015.
- [26] H. G. Bock and K.-J. Plitt, "A Multiple Shooting Algorithm for Direct Solution of Optimal Control Problems," *IFAC Proceedings Volumes*, vol. 17, no. 2, pp. 1603–1608, 1984.
- [27] T. Carraro, M. Geiger, and R. Rannacher, "Indirect Multiple Shooting for Nonlinear Parabolic Optimal Control Problems with Control Constraints," *SIAM Journal on Scientific Computing*, vol. 36, no. 2, pp. A452–A481, 2014.
- [28] M. Geisert and N. Mansard, "Trajectory Generation for Quadrotor Based Systems Using Numerical Optimal Control," in *2016 IEEE International Conference on Robotics and Automation (ICRA)*, pp. 2958–2964, IEEE, 2016.
- [29] M. R. Osborne, "On Shooting Methods for Boundary Value Problems," *Journal of Mathematical Analysis and Applications*, vol. 27, no. 2, pp. 417–433, 1969.
- [30] A. Van Mulders, J. Schoukens, M. Volckaert, and M. Diehl, "Two nonlinear optimization methods for black box identification compared," *Automatica*, vol. 46, pp. 1675–1681, Oct. 2010.

- [31] A. H. Ribeiro and L. A. Aguirre, “Shooting Methods for Parameter Estimation of Output Error Models,” *IFAC-PapersOnLine*, vol. 50, pp. 13998–14003, July 2017.
- [32] J. P. Noël and J. Schoukens, “Grey-box state-space identification of nonlinear mechanical vibrations,” *International Journal of Control*, vol. 91, pp. 1118–1139, May 2018.
- [33] L. Ljung and P. E. Caines, “Asymptotic normality of prediction error estimators for approximate system models,” *Stochastics*, vol. 3, pp. 29–46, Jan. 1980.
- [34] Y. Nesterov, *Introductory Lectures On Convex Programming*. 1998.
- [35] W. Rudin, *Principles of Mathematical Analysis*. International Series in Pure and Applied Mathematics, McGraw-Hill, 1964.
- [36] M. Farina and L. Piroddi, “Some convergence properties of multi-step prediction error identification criteria,” in *2008 47th IEEE Conference on Decision and Control*, pp. 756–761, Dec. 2008.
- [37] J. A. Rossiter and B. Kouvaritakis, “Modelling and implicit modelling for predictive control,” *International Journal of Control*, vol. 74, pp. 1085–1095, Jan. 2001.
- [38] M. Farina and L. Piroddi, “Simulation error minimization identification based on multi-stage prediction,” *International Journal of Adaptive Control and Signal Processing*, vol. 25, no. 5, pp. 389–406, 2011.
- [39] J. Zhao, Y. Zhu, and R. Patwardhan, “Identification of k-step-ahead prediction error model and MPC control,” *Journal of Process Control*, vol. 24, pp. 48–56, Jan. 2014.
- [40] E. Terzi, L. Fagiano, M. Farina, and R. Scattolini, “Learning multi-step prediction models for receding horizon control,” in *2018 European Control Conference (ECC)*, pp. 1335–1340, June 2018.
- [41] M. Lalee, J. Nocedal, and T. Plantenga, “On the Implementation of an Algorithm for Large-Scale Equality Constrained Optimization,” *SIAM Journal on Optimization*, vol. 8, no. 3, pp. 682–706, 1998.
- [42] R. M. May, “Simple mathematical models with very complicated dynamics,” *Nature*, vol. 261, no. 5560, pp. 459–467, 1976.
- [43] Y. LeCun, L. Bottou, G. B. Orr, and K.-R. Müller, “Efficient BackProp,” in *Neural Networks: Tricks of the Trade*, Lecture Notes in Computer Science, pp. 9–50, Springer, Berlin, Heidelberg, 1998.
- [44] A. Dvoretzky, J. Kiefer, and J. Wolfowitz, “Asymptotic Minimax Character of the Sample Distribution Function and of the Classical Multinomial Estimator,” *The Annals of Mathematical Statistics*, vol. 27, pp. 642–669, Sept. 1956.

## A Computing the derivatives

### A.1 Sensitivity equations

Let the Jacobian matrices of  $\mathbf{h}(\mathbf{x}, \mathbf{z}; \boldsymbol{\theta})$  with respect to  $\mathbf{x}$  and to  $\boldsymbol{\theta}$  evaluated at the point  $(\mathbf{x}[k], \mathbf{z}[k]; \boldsymbol{\theta})$  be denoted, respectively, as  $A_k$  and  $B_k$ . Similarly, the Jacobian matrices of  $\mathbf{g}(\mathbf{x}, \mathbf{z}; \boldsymbol{\theta})$  are denoted as  $C_k$  and  $F_k$ . Also, we denote the Jacobian matrices of  $\hat{\mathbf{y}}[k]$  with respect to  $\boldsymbol{\theta}$  and to  $\mathbf{x}_0$  as  $J_{\boldsymbol{\theta}}[k]$  and  $J_{\mathbf{x}_0}[k]$ . And the Jacobian matrices of  $\mathbf{x}[k]$  are denoted as  $D_{\boldsymbol{\theta}}[k]$  and  $D_{\mathbf{x}_0}[k]$ .

A direct application of the chain rule to (2) gives a recursive formula for computing the derivatives of the predicted output in relation to the parameters in the interval  $1 \leq k \leq N$ :

$$\begin{aligned} D_{\boldsymbol{\theta}}[k] &= A_k D_{\boldsymbol{\theta}}[k-1] + B_k \text{ for } D_{\boldsymbol{\theta}}[0] = \mathbf{0} \\ J_{\boldsymbol{\theta}}[k] &= C_k D_{\boldsymbol{\theta}}[k] + F_k. \end{aligned} \quad (\text{A.1})$$

A similar recursive formula may be used for computing the derivatives of the predicted output in relation to the initial conditions:

$$\begin{aligned} D_{\mathbf{x}_0}[k] &= A_k D_{\mathbf{x}_0}[k-1] \text{ for } D_{\mathbf{x}_0}[0] = \mathbf{I} \\ J_{\mathbf{x}_0}[k] &= C_k D_{\mathbf{x}_0}[k]. \end{aligned} \quad (\text{A.2})$$

Finally, we define  $D[k] = [D_{\boldsymbol{\theta}}[k], D_{\mathbf{x}_0}[k]]$  and  $J[k] = [J_{\boldsymbol{\theta}}[k], J_{\mathbf{x}_0}[k]]$ .

### A.2 Single shooting

For the cost function  $V$  defined as in (1), its gradient  $\nabla V$  is given by:

$$\nabla V = \frac{2}{N} \sum_{k=1}^N J[k](\hat{\mathbf{y}}[k] - \mathbf{y}[k]), \quad (\text{A.3})$$

Its Hessian  $\nabla^2 V$  is given by:

$$\nabla^2 V = \frac{2}{N} \sum_{k=1}^N (J[k]^T J[k] + \mathbf{S}[k]). \quad (\text{A.4})$$

where  $\mathbf{S}[k] = \sum_{j=1}^{N_y} \hat{y}_j[k] \nabla^2 \hat{y}_j[k]$ . Ignoring  $\mathbf{S}[k]$  is a common approximation used in least-squares algorithms, that will also be used here when computing derivatives numerically.

### A.3 Multiple shooting

In order to solve the problem using the sequential quadratic programming solver [41] we must be able to compute: i) The cost function  $V^M$ ; ii) its gradient  $\nabla V^M$ ; iii) the constraints; iv) the Jacobian matrix of the constraints (which can be represented using a sparse representation); and, v) for any given vector  $\mathbf{p}$ , the product of the Lagrangian<sup>6</sup> Hessian and the vector  $\mathbf{p}$  (the full Lagrangian Hessian matrix does not need to be computed). The following sequence provides a way of computing all derivatives required by the optimizer.

**Algorithm 1 (Derivatives)** For a given parameter  $\boldsymbol{\theta}$  and set of initial conditions:

<sup>6</sup> The Lagrangian is given by:  $\mathcal{L}(\phi, \boldsymbol{\lambda}) = V(\phi) + \boldsymbol{\lambda}^T \mathbf{c}(\phi)$ .



- (1) For  $i = 1, \dots, M$ , do:
  - (a) For  $k = m_i + 1, \dots, m_{i+1}$ :
    - (i) Compute  $\mathbf{x}^i[k]$  and  $\hat{\mathbf{y}}^i[k]$  with (2).
    - (ii) Compute  $A_k, B_k, C_k$  and  $F_k$ .
    - (iii) Compute  $D^i[k]$  and  $J^i[k]$  with the sensitivity equations.
  - (b) Compute  $V_i$  using Eq. (10).
  - (c) Compute  $\nabla V_i$  using a formula equivalent to (A.3).
  - (d) Approximate the product of the Hessian with a given vector,  $\nabla^2 V_i \mathbf{p}$ , using the first terms from a expression equivalent to (A.4)
- (2) Compute  $V^M$  with (11);
- (3) Compute  $\nabla V^M = \sum_{i=1}^M \frac{\Delta m_i}{N} \nabla V_i$ ;
- (4) Compute the value of the constraint from the values of  $\mathbf{x}^i[m_{i+1}]$ ,  $i = 1, \dots, M$ ;
- (5) Compute the Jacobian matrix of the constraints from  $J^i[m_{i+1}]$ ,  $i = 1, \dots, M$ ;
- (6) Compute  $\nabla^2 V^M \mathbf{p} = \sum_{i=1}^M \frac{\Delta m_i}{N} \nabla^2 V_i \mathbf{p}$ ;
- (7) Compute the product of the Hessian  $\lambda^T \mathbf{c}(\phi)$  with a vector  $\mathbf{p}$  using 2-point finite differences;
- (8) Compute the product of the Lagrangian Hessian and a vector  $\nabla^2 \mathcal{L}(\phi, \lambda) \mathbf{p}$ , summing the Hessians computed in steps 6 and 7.

Some approximations were used for computing the second derivatives: 1) for computing the Hessian of the objective function, the standard least-squares approximation for the Hessian is used; and, 2) for computing the Hessian of the constraint we use finite-difference approximation. The use of finite differences here comes inexpensively because we only need to evaluate the Hessian times a vector, and not the full matrix. Hence, it can be done at the cost of an extra Jacobian matrix evaluation.

Notice that step (1) from the above algorithm can be parallelized, with different processes (or threads) performing the computation for different values of  $i$ .

## B Proofs

### B.1 Preliminary results

**Lemma 5** Let  $\mathbf{f}$  and  $\mathbf{g}$  be two Lipschitz functions on  $\Omega$  with constants  $L_f$  and  $L_g$ . Then,

- a)  $\mathbf{f} + \mathbf{g}$  is also a Lipschitz function on  $\Omega$  with Lipschitz constant upper bounded by  $(L_f + L_g)$ ;
- b) if, additionally,  $\mathbf{f}$  and  $\mathbf{g}$  are bounded by  $M_f$  and  $M_g$  on  $\Omega$ , then  $\mathbf{fg}$  is also a Lipschitz function on  $\Omega$  with Lipschitz constant upper bounded by  $(L_f M_g + L_g M_f)$ .

### B.2 Proof of Theorem 1 (a)

Let us call:

$$\|\Delta \hat{\mathbf{y}}[k]\| = \|\mathbf{g}(\mathbf{x}[k], \mathbf{z}[k]; \boldsymbol{\theta}) - \mathbf{g}(\mathbf{w}[k], \mathbf{z}[k]; \boldsymbol{\phi})\|. \quad (\text{B.1})$$

Because  $\mathbf{h}$  and  $\mathbf{g}$  are Lipschitz in  $(\mathbf{x}, \boldsymbol{\theta})$  we have:

$$\begin{aligned} \|\mathbf{h}(\mathbf{x}, \mathbf{z}, \boldsymbol{\theta}) - \mathbf{h}(\mathbf{w}, \mathbf{z}, \boldsymbol{\phi})\|^2 &\leq L_h^2 (\|\mathbf{x} - \mathbf{w}\|^2 + \|\boldsymbol{\theta} - \boldsymbol{\phi}\|^2), \\ \|\mathbf{g}(\mathbf{x}, \mathbf{z}, \boldsymbol{\theta}) - \mathbf{g}(\mathbf{w}, \mathbf{z}, \boldsymbol{\phi})\|^2 &\leq L_g^2 (\|\mathbf{x} - \mathbf{w}\|^2 + \|\boldsymbol{\theta} - \boldsymbol{\phi}\|^2), \end{aligned}$$

for all  $(\mathbf{x}, \mathbf{z}, \boldsymbol{\theta})$  and  $(\mathbf{w}, \mathbf{z}, \boldsymbol{\phi})$  in  $(\Omega_{\mathbf{x}}, \Omega_{\mathbf{z}}, \Omega_{\boldsymbol{\theta}})$ . Applying these relations recursively we get that:

$$\|\Delta \hat{\mathbf{y}}[k]\|^2 \leq L_g^2 L_h^{2k} \|\mathbf{x}_0 - \mathbf{w}_0\|^2 + L_g^2 \left( \sum_{\ell=0}^k L_h^{2\ell} \right) \|\boldsymbol{\theta} - \boldsymbol{\phi}\|^2.$$

Since  $L_h$  is positive, the constant multiplying the second term in the above equation is always larger than constant multiplying the first one. Hence, taking the square root on both sides of the above inequality and after simple manipulations, we get:

$$\|\Delta \hat{\mathbf{y}}[k]\| \leq L_g S(k) \|\boldsymbol{\theta}, \mathbf{x}_0\|^T - [\boldsymbol{\phi}, \mathbf{w}_0]^T. \quad (\text{B.2})$$

where:

$$S(k) = \sqrt{\sum_{\ell=0}^k L_h^{2\ell}} = \begin{cases} \sqrt{k+1} & \text{if } L_h = 1 \\ \sqrt{\frac{L_h^{2k+2} - 1}{L_h^2 - 1}} & \text{if } L_h \neq 1. \end{cases} \quad (\text{B.3})$$

Since  $\Omega$  is compact and  $\hat{\mathbf{y}}[k]$  is a (Lipschitz) continuous function of the parameters and initial conditions, then  $\hat{\mathbf{y}}[k]$  is bounded in  $\Omega$ , i.e.  $\|\hat{\mathbf{y}}[k]\| \leq M(k)$ . And, it follows from (B.2) and from the existence of an invariant set<sup>7</sup> in  $\Omega$  that  $M(k) = \mathcal{O}(S(k))$ .

The following inequality follows from (1):

$$|V(\boldsymbol{\theta}, \mathbf{x}_0) - V(\boldsymbol{\phi}, \mathbf{w}_0)| \leq \frac{2}{N} \sum_{k=1}^N (L_y + M(k)) \|\Delta \hat{\mathbf{y}}[k]\|, \quad (\text{B.4})$$

where  $L_y = \max_{1 \leq k \leq N} \|\mathbf{y}[k]\|$ . And, by putting together (B.4) and (B.2):

$$|V(\boldsymbol{\theta}, \mathbf{x}_0) - V(\boldsymbol{\phi}, \mathbf{w}_0)| \leq L_{V_1} \|\mathbf{x}_0, \boldsymbol{\theta}\|^T - [\mathbf{w}_0, \boldsymbol{\phi}]^T\|,$$

<sup>7</sup> There are multiple ways to guarantee the invariant set premise will hold, but a very simple way is to just choose  $\mathbf{h}$  such that  $\mathbf{h}(\mathbf{0}, \mathbf{z}; \mathbf{0}) = \mathbf{0}$ . In this case,  $\{\mathbf{0}\}$  is an invariant set and if  $\Omega_{\boldsymbol{\theta}}$  contain this point the premise is satisfied. For this specific case, one can just choose  $[\boldsymbol{\phi}, \mathbf{w}_0] = \mathbf{0}$  and it follows from (B.2) that  $\|\hat{\mathbf{y}}[k]\| \leq L_g S(k) \|\boldsymbol{\theta}, \mathbf{x}_0\| = \mathcal{O}(S(k))$ . The more general case, for any invariant set, follows from a similar deduction.



for  $L_V = \left( \frac{2L_g}{N} \sum_{k=1}^N (L_y + M(k))S(k) \right)$ . The asymptotic analysis of this expression with regard to  $N$  yields (7).

### B.3 Proof of Theorem 1 (b)

It follows from (A.3) that:

$$\|\nabla V(\boldsymbol{\theta}, \mathbf{x}_0) - \nabla V(\boldsymbol{\phi}, \mathbf{w}_0)\| \leq \frac{2}{N} \sum_{k=1}^N L_y \|\Delta J[k]\| + \|\Delta(J[k]\hat{\mathbf{y}}[k])\|, \quad (\text{B.5})$$

where we have used the notation  $\Delta J[k]$  to denote the difference between  $J[k]$  evaluated at  $(\boldsymbol{\theta}, \mathbf{x}_0)$  and  $(\boldsymbol{\phi}, \mathbf{w}_0)$ . Analogously,  $\Delta(J[k]\hat{\mathbf{y}}[k])$  denote the difference between  $J[k]\hat{\mathbf{y}}[k]$  evaluated at the two distinct points.

From equation (A.1) and (A.2) it follows that:

$$J_{\boldsymbol{\theta}}[k] = C_k \sum_{\ell=1}^k \left( \prod_{j=1}^{k-\ell} A_{k-j+1} \right) B_{\ell} + F_k; \quad J_{\mathbf{x}_0}[k] = C_k \prod_{\ell=1}^k A_{k-\ell+1}. \quad (\text{B.6})$$

Since, the Jacobian of  $\mathbf{h}$  is Lipschitz with Lipschitz constant  $L'_h$ , it follows that:

$$\|\Delta A_j\|^2 \leq (L'_h)^2 (\|\mathbf{x}[j] - \mathbf{w}[j]\|^2 + \|\boldsymbol{\theta} - \boldsymbol{\phi}\|^2). \quad (\text{B.7})$$

Using a procedure analogous to the one used to get Equation (B.2), it follows that:

$$\|\Delta A_j\| \leq L'_h S(j) \|\boldsymbol{\theta}, \mathbf{x}_0\|^T - [\boldsymbol{\phi}, \mathbf{w}_0]^T\|, \quad (\text{B.8})$$

where  $S(j)$  is defined as in (B.3). An identical formula holds for  $B_j$  and a similar formula, replacing  $L'_h$  with  $L'_g$ , holds for  $C_j$  and  $F_j$ .

Since  $\mathbf{h}$  and  $\mathbf{g}$  are Lipschitz with Lipschitz constants  $L_h$  and  $L_g$  it follows that  $\|A_j\| \leq L_h$ ,  $\|B_j\| \leq L_h$ ,  $\|C_j\| \leq L_g$  and  $\|D_j\| \leq L_g$ . Hence, it follows from (B.2), (B.6), (B.8) and the repetitive application of Lemma 5 that  $\|\Delta J_{\boldsymbol{\theta}}[k]\|$ ,  $\|\Delta J_{\mathbf{x}_0}[k]\|$ ,  $\|\Delta(J_{\boldsymbol{\theta}}[k]\hat{\mathbf{y}}[k])\|$  and  $\|\Delta(J_{\mathbf{x}_0}[k]\hat{\mathbf{y}}[k])\|$  are upper bounded by  $\|\boldsymbol{\theta}, \mathbf{x}_0\|^T - [\boldsymbol{\phi}, \mathbf{w}_0]^T\|$  multiplied by the following constants:

$$L_{J_{\boldsymbol{\theta}}}(k) = \sum_{\ell=1}^k P(k, \ell) + L'_g S(k); \quad L_{J_{\mathbf{x}_0}}(k) = P(k, 1)$$

$$L_{J_{\boldsymbol{\theta}}\hat{\mathbf{y}}}(k) = \sum_{\ell=1}^k Q(k, \ell) + T(k)S(k); \quad L_{J_{\mathbf{x}_0}\hat{\mathbf{y}}}(k) = Q(k, 1),$$

where  $T(k) = (L'_g M(k) + L_g^2)$  and:

$$P(k, \ell) = L_h^{k-\ell} \left( L_g L'_h \sum_{j=\ell}^k S(j) + L_h L'_g S(k) \right)$$

$$Q(k, \ell) = L_h^{k-\ell} \left( M(k) L_g L'_h \sum_{j=\ell}^k S(j) + L_h T(k) S(k) \right).$$

Hence,

$$\|\nabla V(\boldsymbol{\theta}, \mathbf{x}_0) - \nabla V(\boldsymbol{\phi}, \mathbf{w}_0)\| \leq L'_V \|\boldsymbol{\theta}, \mathbf{x}_0\|^T - [\boldsymbol{\phi}, \mathbf{w}_0]^T\|,$$

where

$$L'_V = \frac{2}{N} \sum_{k=1}^N \left( L_y (L_{J_{\boldsymbol{\theta}}}(k) + L_{J_{\mathbf{x}_0}}(k)) + L_{J_{\boldsymbol{\theta}}\hat{\mathbf{y}}}(k) + L_{J_{\boldsymbol{\theta}}\hat{\mathbf{y}}}(k) \right).$$

Putting everything together the asymptotic analysis of  $L'_V$  results in (8).